STM JOURNALS

Research and Reviews: Journal of Physics
ISSN: 2278–2265(online), ISSN: 2347-9973(print)
Volume 5, Issue 3
www.stmjournals.com

Stress Analysis of Rotating Cylindrical Pressure Vessel of Functionally Graded Material by Element Based Material Gradation

Amit Kumar Thawait*
Department of Mechanical Engineering, Shri Shankaracharya Group of Institutes, Bhilai, Chhattisgarh, India

Abstract

The present study aims at the elastic analysis of rotating cylindrical pressure vessels made of functionally graded materials (FGMs), by element based gradation. Material properties of the shells vary in radial direction according to exponential distribution law. Ceramic-metal and metal-ceramic, both the types of FGM are considered and the effects of gradation of material properties on stress and deformation behavior of the shells are investigated. Further, a comparison of deformation and stresses for different values of thickness parameters in ceramic-metal and metal-ceramic shell is made. Results obtained show that there is a significant variation in stresses and deformation behavior of the FGM shells for different values of thickness parameter.

Keywords: *Functionally graded material (FGM), elastic stress analysis, cylindrical pressure vessel, rotating shell, element based material gradation*

****Author for Correspondence*** E-mail: amkthawait@gmail.com

INTRODUCTION

Functionally graded materials (FGMs) are special composite materials that have continuous and smooth spatial variations of physical and mechanical properties. The gradation of material properties in FGMs is achieved by varying the volume fractions of the constituents. Functionally graded shells are widely used in space vehicles, aircrafts, nuclear power plants and many other engineering applications [1]. The total stresses due to internal pressure and centrifugal load have effects on their strength and safety. Thus, control and optimization of total stresses and displacement fields is an important task, which is achieved by varying the material property in FGM pressure vessels.

Many researchers have worked on elastic analysis of rotating conical shells, cylindrical shells, disks etc. by analytical as well as approximate methods such as finite element method. Tutuncu *et al.* reported closed form solution for stresses and displacements in functionally graded cylindrical and spherical vessels subjected to internal pressure, using the infinitesimal theory of elasticity [2]. The material stiffness obeying a power law is assumed to vary through the wall thickness and Poisson's ratio is assumed constant. Abrinia *et al.* have analyzed FGM thick cylinders under combined pressure and temperature loading [3]. Nejad *et al.* reported work on stresses analysis in isotropic rotating thick-walled cylindrical pressure vessels made of functionally graded materials [4]. The pressure, inner radius and outer radius are considered constant. Material properties are considered as a function of the radius of the cylinder to a power law function and the Poisson's ratio is assumed as constant.

Finite element method based on Rayleigh-Ritz energy formulation is applied to obtain the elastic behavior of functionally graded thick truncated conical shell by Asemi *et al.* [5]. Using this method, the effects of semi-vertex angle of the cone and the power law exponent on distribution of different types of displacements and stresses are considered. In a recent work, Sadrabadi *et al.* studied thick walled cylindrical tanks or tubes made of functionally graded material, under internal pressure and temperature gradient [6].

Material parameters have been considered as power functions. Ghannad *et al.* worked on elastic analysis of pressurized thick cylindrical shells with variable thickness made of functionally graded materials [7].

Nejad *et al.* have performed a semi analytical approach using first-order shear deformation theory (FSDT), matched asymptotic method (MAM) and multilayer method (MLM), for the purpose of elastic analysis of rotating thick truncated conical shells made of functionally graded materials (FGMs) [1, 8, 9]. The cone has finite length, and it is subjected to axisymmetric hydrostatic internal pressure. The inner surface of the cone is pure ceramic and the outer surface is pure metal, and the material composition varies continuously along its thickness.

In present research work, hollow rotating cylindrical pressure vessels subjected to internal pressure are analyzed. Governing equations are derived by principle of stationary total potential. The shells are made of functionally graded material of aluminum metal and zirconia ceramic. Functional gradation of the material properties is done by exponential law using element-based gradation.

The work aims at investigating the effects of functional gradation of the material properties on the deformation and stresses behavior of the shells for both, ceramic-metal and metal-ceramic FGM. Further, the effect of thickness parameter is also found out and presented in the form of graph for some numerical problems.

MATERIAL MODELING

Young's modulus and density of the disk are assumed to vary exponentially along radial direction as [10]:

$$E(r) = E_0 e^{\beta r} \tag{1}$$

$$\rho(r) = \rho_0 e^{\gamma r} \tag{2}$$

$$E_0 = E_A e^{-\beta a} \tag{3}$$

$$\rho_0 = \rho_A e^{-\gamma a} \tag{4}$$

$$\gamma = \frac{1}{a-b} ln\left(\frac{\rho_A}{\rho_B}\right) \tag{5}$$

$$\beta = \frac{1}{a-b} ln\left(\frac{E_A}{E_B}\right) \tag{6}$$

$E(r)$ and $\rho(r)$ are modulus of elasticity and density at radius r; E_A, E_B and ρ_A, ρ_B are modulus of elasticity and density at the inner and outer radius respectively.

FINITE ELEMENT MODELING

The rotating cylinders are modeled as a plane strain axisymmetric problem (Figure 1). The element displacement vector $\{\varphi\}$ can be obtained as:

$$\{\varphi\} = \{u \quad v\}^T = [N]\{\delta\} \tag{7}$$

Where, $[N]$ is the matrix of shape functions and $\{\delta\}$ is nodal displacement vector. For quadratic quadrilateral element, $[N]$ and $\{\delta\}$ are given as:

$$[N] = \begin{bmatrix} N_1 & 0 & N_2 & 0 & \dots & \dots & N_8 & 0 \\ 0 & N_1 & 0 & N_2 & \dots & \dots & 0 & N_8 \end{bmatrix}$$

$$\{\delta\} = \{u_1 \quad v_1 \quad u_2 \quad v_2 \quad \dots \quad \dots \quad u_8 \quad v_8\}^T$$

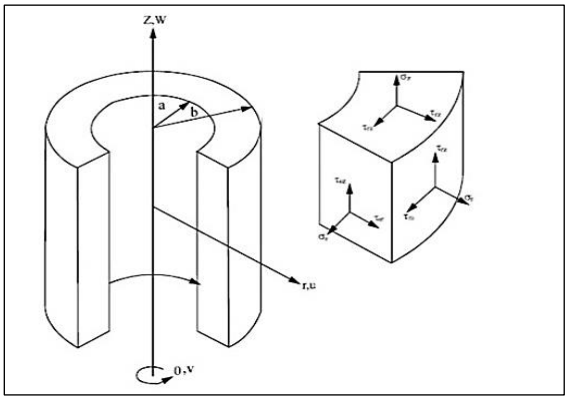

Fig. 1: *Cylindrical Geometry and Stresses on a Cylindrical Element.*

In natural co-ordinates (ξ-η), the shape functions are given as [11]:

$$N_1 = \left(\frac{1}{4}\right)(1-\xi)(1-\eta)(-1-\xi-\eta)$$

$$N_2 = \left(\frac{1}{4}\right)(1+\xi)(1-\eta)(-1+\xi-\eta)$$

$$N_3 = \left(\frac{1}{4}\right)(1+\xi)(1+\eta)(-1+\xi+\eta)$$

$$N_4 = \left(\frac{1}{4}\right)(1-\xi)(1+\eta)(-1-\xi+\eta)$$

$$N_5 = \left(\frac{1}{2}\right)(1-\xi^2)(1-\eta)$$

$$N_6 = \left(\frac{1}{2}\right)(1+\xi)(1-\eta^2)$$

$$N_7 = \left(\frac{1}{2}\right)(1-\xi^2)(1+\eta)$$

$$N_8 = \left(\frac{1}{2}\right)(1-\xi)(1-\eta^2)$$

The strain components are related to elemental displacement components as [11]:

$$\{\varepsilon\} = \{\varepsilon_r \quad \varepsilon_\theta \quad \varepsilon_z \quad \gamma_{rz}\}^T = \left\{\frac{\partial u}{\partial r} \quad \frac{u}{r} \quad \frac{\partial v}{\partial z} \quad \frac{\partial u}{\partial z} + \frac{\partial v}{\partial r}\right\}^T \tag{8}$$

$$\left\{\frac{\partial u}{\partial r} \quad \frac{u}{r} \quad \frac{\partial v}{\partial z} \quad \frac{\partial u}{\partial z} + \frac{\partial v}{\partial r}\right\}^T = [B_1]\left\{\frac{\partial u}{\partial r} \quad \frac{\partial u}{\partial z} \quad \frac{\partial v}{\partial r} \quad \frac{\partial v}{\partial z} \quad \frac{u}{r}\right\}^T \tag{9}$$

Where, ε_r, ε_θ, ε_z and Υ_{rz} are radial, tangential, axial and shear strain respectively. By transforming the global co-ordinates into natural co-ordinates (ξ-η),

$$\left\{\frac{\partial u}{\partial r} \quad \frac{\partial u}{\partial z} \quad \frac{\partial v}{\partial r} \quad \frac{\partial v}{\partial z} \quad \frac{u}{r}\right\}^T = [B_2]\left\{\frac{\partial u}{\partial \xi} \quad \frac{\partial u}{\partial \eta} \quad \frac{\partial v}{\partial \xi} \quad \frac{\partial v}{\partial \eta} \quad \frac{u}{r}\right\}^T \tag{10}$$

$$\left\{\frac{\partial u}{\partial \xi} \quad \frac{\partial u}{\partial \eta} \quad \frac{\partial v}{\partial \xi} \quad \frac{\partial v}{\partial \eta} \quad \frac{u}{r}\right\}^T = [B_3]\{u_1 \quad v_1 \quad u_2 \quad v_2 \quad \ldots \quad \ldots \quad u_8 \quad v_8\}^T \tag{11}$$

The above elemental strain-displacement relationships can be written as:

$$\{\varepsilon\} = [B]\{\delta\}^e \tag{12}$$

Where [B] is strain-displacement relationship matrix, which contains derivatives of shape functions. For a quadratic quadrilateral element, it is calculated as:

$$[B] = [B_1] \times [B_2] \times [B_3] \tag{13}$$

$$[B_1] = \begin{bmatrix} 1 & 0 & 0 & 0 & 0 \\ 0 & 0 & 0 & 0 & 1 \\ 0 & 0 & 0 & 1 & 0 \\ 0 & 1 & 1 & 0 & 0 \end{bmatrix}$$

$$[B_2]=\begin{bmatrix} \frac{J_{22}}{|J|} & \frac{-J_{12}}{|J|} & 0 & 0 & 0 \\ \frac{-J_{21}}{|J|} & \frac{J_{11}}{|J|} & 0 & 0 & 0 \\ 0 & 0 & \frac{J_{22}}{|J|} & \frac{-J_{12}}{|J|} & 0 \\ 0 & 0 & \frac{-J_{21}}{|J|} & \frac{J_{11}}{|J|} & 0 \\ 0 & 0 & 0 & 0 & 1 \end{bmatrix}$$

$$[B_3]=\begin{bmatrix} \frac{\partial N_1}{\partial \xi} & 0 & \frac{\partial N_2}{\partial \xi} & 0 & \dots & \dots & \frac{\partial N_8}{\partial \xi} & 0 \\ \frac{\partial N_1}{\partial \eta} & 0 & \frac{\partial N_2}{\partial \eta} & 0 & \dots & \dots & \frac{\partial N_8}{\partial \eta} & 0 \\ 0 & \frac{\partial N_1}{\partial \xi} & 0 & \frac{\partial N_2}{\partial \xi} & \dots & \dots & 0 & \frac{\partial N_8}{\partial \xi} \\ 0 & \frac{\partial N_1}{\partial \eta} & 0 & \frac{\partial N_2}{\partial \eta} & \dots & \dots & 0 & \frac{\partial N_8}{\partial \eta} \\ \frac{N_1}{r} & 0 & \frac{N_2}{r} & 0 & \dots & \dots & \frac{N_8}{r} & 0 \end{bmatrix}$$

Where, *J* is the Jacobian matrix, used to transform the global co-ordinates into natural co-ordinates. It is given as:

$$[J]=\begin{bmatrix} \sum_{i=1}^{8}\frac{\partial N_i}{\partial \xi} r_i & \sum_{i=1}^{8}\frac{\partial N_i}{\partial \xi} z_i \\ \sum_{i=1}^{8}\frac{\partial N_i}{\partial \eta} r_i & \sum_{i=1}^{8}\frac{\partial N_i}{\partial \eta} z_i \end{bmatrix}$$

From Hooks law, components of stresses in radial, circumferential and axial directions are related to components of total strain as:

$$\varepsilon_r = \frac{1}{E}\left(\sigma_r - \nu\sigma_\theta - \nu\sigma_z\right) \tag{14}$$

$$\varepsilon_\theta = \frac{1}{E}\left(\sigma_\theta - \nu\sigma_r - \nu\sigma_z\right) \tag{15}$$

$$\varepsilon_z = \frac{1}{E}\left(\sigma_z - \nu\sigma_\theta - \nu\sigma_r\right) \tag{16}$$

By solving above equations, stress strain relationship can be obtained as follows:

$$\sigma_r = \frac{E(r)}{(1-2\nu)(1+2\nu)}\left[(1-\nu)\varepsilon_r + \nu\varepsilon_z + \nu\varepsilon_\theta\right] \tag{17}$$

Similarly, axial and circumferential stresses can also be obtained.
In standard finite element matrix notation, above stress strain relations can be written as:

$$\{\sigma\} = \left[D(r)\right]\{\varepsilon\} \tag{18}$$

Where,

$$\{\sigma\} = \{\sigma_r \quad \sigma_\theta \quad \sigma_z \quad \tau_{rz}\}^T$$

$$\{\varepsilon\} = \{\varepsilon_r \quad \varepsilon_\theta \quad \varepsilon_z \quad \gamma_{rz}\}^T$$

$$D(r) = \frac{(1-\nu)E(r)}{(1+\nu)(1-2\nu)} \begin{bmatrix} 1 & \frac{\nu}{(1-\nu)} & \frac{\nu}{(1-\nu)} & 0 \\ \frac{\nu}{(1-\nu)} & 1 & \frac{\nu}{(1-\nu)} & 0 \\ \frac{\nu}{(1-\nu)} & \frac{\nu}{(1-\nu)} & 1 & 0 \\ 0 & 0 & 0 & \frac{1-2\nu}{2(1-\nu)} \end{bmatrix}$$

Upon rotation, the shell experiences a body force which under constrained boundary, results in deformation and stores internal strain energy *U*.

$$U = \frac{1}{2}\int_V \{\varepsilon\}^T \{\sigma\}\, dv \tag{19}$$

The work potential due to body and surface forces, resulting from centrifugal action and internal pressure is given by:

$$V = -\int_v \{\delta\}^T \{q_v\}\, dv - \int_s \{\delta\}^T \{q_s\}\, ds \tag{20}$$

Upon substituting Eqs. (12) and (18) in Eqs. (19) and (20); the elemental strain energy and work potential are given by:

$$U^e = \pi \iint \{\delta\}^{eT} [B]^T [D(r)][B]\{\delta\}^e\, r dz dr \tag{21}$$

$$V^e = -2\pi \iint \{\delta\}^{eT} [N]^T \{q_v\} r\, dz dr - 2\pi r_i \int \{\delta\}^{eT} [N]^T \{q_s\}\, dz \tag{22}$$

For a cylindrical shell rotating at ω rad/sec and subjected to internal pressure *P*, the body and surface force vectors for each element are given as:

$$\{q_v\} = \begin{Bmatrix} \rho(r)\omega^2 r \\ 0 \end{Bmatrix}$$

$$\{q_s\} = \begin{Bmatrix} P_x \\ 0 \end{Bmatrix}$$

The total potential of the element is obtained from Eqs. (21) and (22) as:

$$\pi_p{}^e = \frac{1}{2}\{\delta\}^{eT} [K]^e \{\delta\}^e - \{\delta\}^{eT} \{f\}^e \tag{23}$$

Here, defining element stiffness matrix $[K]^e$ and element load vector $\{f\}^e$ as:

$$[K]^e = 2\pi \iint [B]^T [D(r)][B]\, r dz dr \tag{24}$$

$$\{f\}^e = 2\pi \iint [N]^T \{q_v\} r\, dz dr + 2\pi r_i \int [N]^T \{q_s\}\, dz \tag{25}$$

In FEM, the functional grading is popularly carried out by assigning the average material properties over a given geometry followed by adhering the geometries thus resulting into layered functional grading of material properties. The downside of this approach is that it yields singular field variable values at the boundaries of the glued geometries. To get better results, it is an established practice to divide the total geometry into very fine geometries. However, a better approach is to assign the average material properties to the elements of mesh of the single geometry.

This is, in other words, better described as assigning material properties to the finite elements instead of geometry. In Eq. (18), the [*D*(*r*)] matrix, being a function of r, is calculated numerically at each node and this results into continuous material property variation throughout the geometry. The element matrices are then assembled to yield the global stiffness matrix and global load vector respectively. The element based grading of material property yields an appropriate approach of functional grading as the shape functions in the elemental formulations being co-ordinate functions make it easier to implement the same [12].

$$\phi^e = \sum_{i=1}^{8} \phi_i N_i \tag{26}$$

Where ϕ^e is element material property, ϕ_i is material property at node *i* and N_i is the shape function.

Total potential energy of the shell is given by:

$$\pi_p = \sum \pi_p{}^e = \frac{1}{2}\{\delta\}^T [K]\{\delta\} - \{\delta\}^T \{F\} \tag{27}$$

Where,

$[K] = \sum_{n=1}^{N} [K]^e$ = Global stiffness matrix,

$\{F\} = \sum_{n=1}^{N} [f]^e$ = global load vector, and

N= No. of elements.

Using the principle of stationary total potential (PSTP), the total potential is set to be stationary with respect to small variation in the nodal degree of freedom, that is:

$$\frac{\partial \pi_p}{\partial \{\delta\}^T} = 0 \tag{28}$$

From above, the system of simultaneous equations is obtained as follows:

$$[K]\{\delta\} = \{F\} \tag{29}$$

RESULTS AND DISCUSSION

Validation

To validate the current work, problems referred by Tutuncu and Ozturk are reconsidered and two types of material models are analyzed [2]. Following equations are used for material modelling in the said reference [2]:

$$V_c = \left(\frac{x-1}{k-1}\right)^n \tag{30}$$

$$\nu = \nu_c V_c + \nu_m (1 - V_c) \tag{31}$$

$$E = E_c V_c + E_m (1 - V_c) \tag{32}$$

Where, *V* is the volume fraction, *E* is young's modulus and *v* is Poisson's ratio, subscript '*m*' refers to metal and '*c*' refers to ceramic. *x* is non-dimensional radius that is *r*/*a* and *k* is the ratio of outer diameter to inner diameter.

In model 1, Poisson's ratio is taken constant (0.333) and young's modulus varies according to Eq. (32) taking *n*=1; while in model 2, both Poisson's ratio and young's modulus vary according to Eqs. (31) and (32) taking *n*=*k*=2. Material properties of the metal and ceramic used are: E_m=200 GPa, E_c=360 GPa, ν_m=0.333, ν_c=0.2 and the vessels are subjected to unit internal pressure that is 1 GPa (Figure 2).

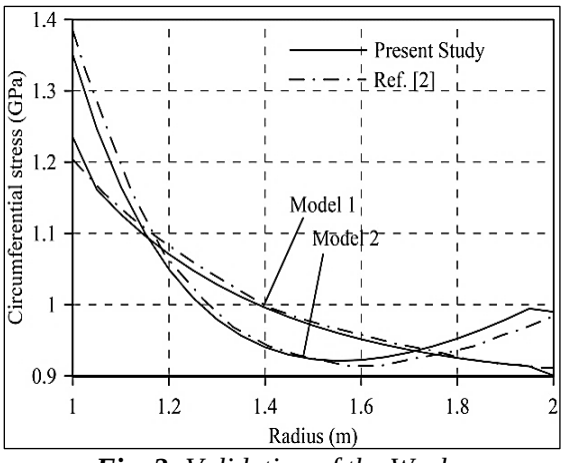

Fig. 2: *Validation of the Work.*

Numerical Results

In this section, some numerical problems of rotating FGM cylindrical pressure vessels are analyzed and the effect of thickness parameter *b/a* on stress and deformation states is found out. Shells have same geometric parameters as above and rotating with an angular velocity of 200 rad/s, subjected to unit internal pressure. Material is modelled by exponential law as discussed in previous section, for which properties used are as [13]:

E_m=70 GPa, E_c=151 GPa, and ν=0.3.

Figures 3–6 show the distribution of radial displacement, radial stress, circumferential stress and von Mises stress respectively along radial direction for ceramic-metal FGM shells while Figures 7–10 show the same for metal-ceramic shells. From Figure 3 and 7, it can be seen that FGM shell having *b/a*=2 has maximum radial displacement and the FGM shell having *b/a*=3 has minimum radial displacement. Radial displacement decreases with increase in *b/a* ratio. It is minimum at the outer radius and maximum at the inner radius for all the shells. By comparing both, the ceramic-metal and metal-ceramic FGM, it is observed that ceramic-metal shell having *b/a*=3, has least radial displacement.

It is observed that radial stress is maximum that is equal to applied internal pressure at inner radius and minimum equals to 0 at outer radius. It is also observed that here the effect of rotation is negligible as compared to applied internal pressure; and radial stresses are complete compressive stresses. It decreases with increase in *b/a.* Circumferential stress is complete positive, means tensile in nature. It is least for *b/a*=3 and maximum for *b/a*=2.

Circumferential stress is maximum at inner radius and minimum at outer radius for all values of *b/a*. von Mises stress is also maximum at inner radius and minimum at outer radius having same distribution as circumferential stress in both metal-ceramic and ceramic-metal FGM. Metal-ceramic FGM shell having *b/a*=3 has the least von Mises stress.

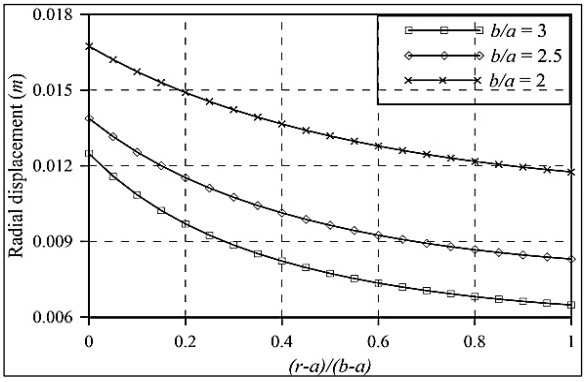

Fig. 3: *Radial Displacement Distribution (Ceramic-Metal FGM).*

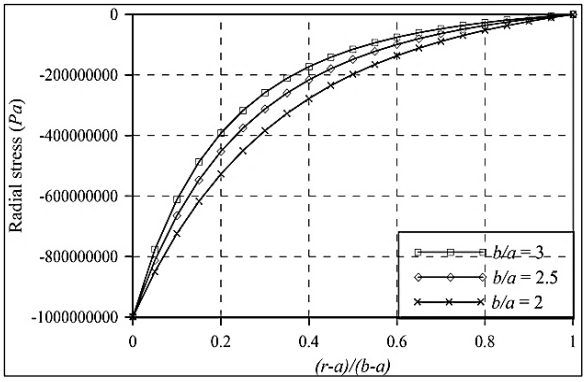

Fig. 4: *Radial Stress Distribution (Ceramic-Metal FGM).*

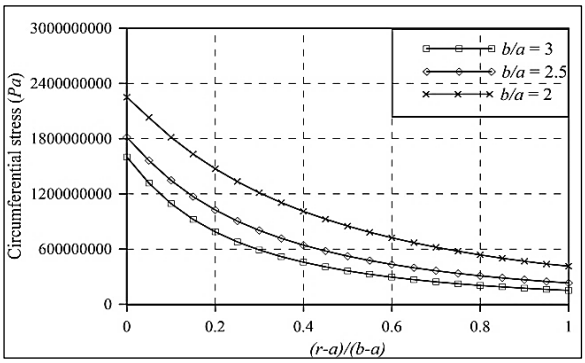

Fig. 5: *Circumferential Stress Distribution (Ceramic-Metal FGM).*

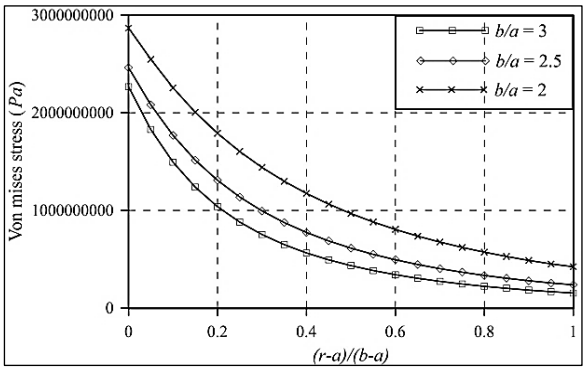

Fig. 6: *von Mises Stress Distribution (Ceramic-Metal FGM).*

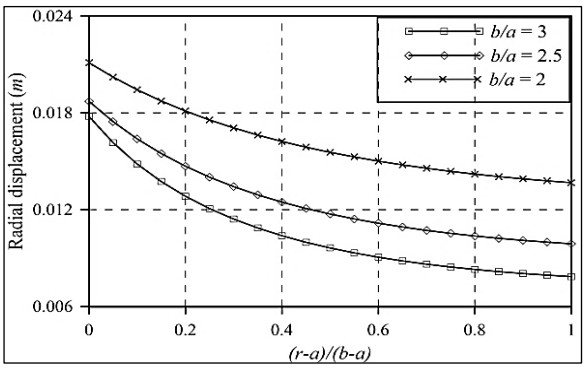

Fig. 7: *Radial Displacement Distribution (Metal-Ceramic FGM).*

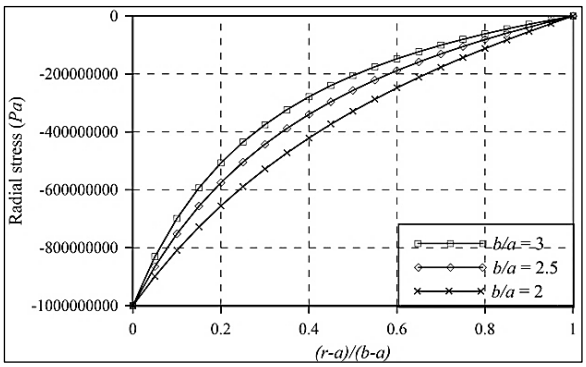

Fig. 8: *Radial Stress Distribution (Metal-Ceramic FGM).*

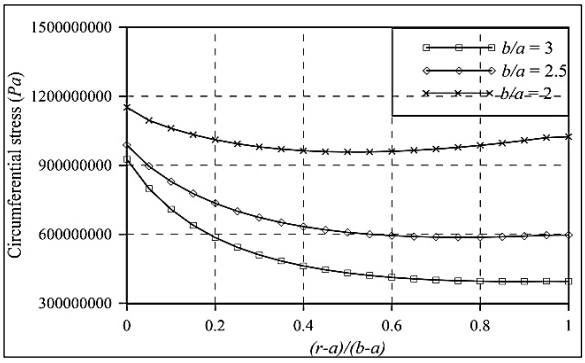

Fig. 9: *Circumferential Stress Distribution (Metal-Ceramic FGM).*

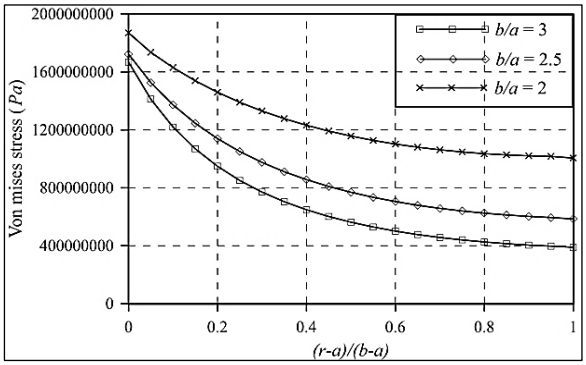

Fig. 10: *von Mises Stress Distribution (Metal-Ceramic FGM).*

By comparing all the stresses, it is observed that von Mises stress is maximum as compared to radial and circumferential stress. Therefore, von Mises stress should be taken as limit stress criteria for rotating cylindrical pressure vessels.

CONCLUSION

The present work proposes a study of rotating FGM cylindrical pressure vessel using element based material gradation. Functional gradation of the material properties is achieved by exponential law. Material properties of aluminum metal and zirconia ceramic are used and metal-ceramic as well as ceramic-metal, both the types of FGM are considered. Principle of stationary total potential (PSTP) is used to derive the governing equation. The results obtained show that stresses and deformation decreases with increasing *b/a* ratio in both, the ceramic-metal and metal-ceramic FGM.

REFERENCES

1. Nejad MZ, Jabbari M, Ghannad M. Elastic Analysis of FGM Rotating Thick Truncated Conical Shells with Axially-Varying Properties under Non-Uniform Pressure Loading. *Compos Struct*. 2015; 122: 561–569p.
2. Tutuncu N, Ozturk M. Exact Solutions for Stresses in Functionally Graded Pressure Vessels. *Compos Part B.* 2001; 32: 683–686p.
3. Abrinia K, Naee H, Sadeghi F, *et al*. New Analysis for the FGM Thick Cylinders under Combined Pressure and Temperature Loading. *Am J Appl Sci*. 2008; 5(7): 852–859p.
4. Nejad MZ, Rahimi GH. Elastic Analysis of FGM Rotating Cylindrical Pressure Vessel. *J Chinese Inst Engrs*. 2010; 33(4): 525–530p.
5. Asemi K, Akhlaghi M, Salehi M, *et al.* Analysis of Functionally Graded Thick Truncated Cone with Finite Length under Hydrostatic Internal Pressure. *Arch Appl Mech.* 2011; 81: 1063–1074p.
6. Sadrabadi SA, Rahimi GH. Yield Onset of Thermo-Mechanical Loading of FGM Thick Walled Cylindrical Pressure Vessels. *International Journal of Mechanical, Aerospace, Industrial,*

Mechatronic and Manufacturing Engineering. 2014; 8(7): 1325–1329p.
7. Ghannad M, Rahimi GH, Nejad MZ. Elastic Analysis of Pressurized Thick Cylindrical Shells with Variable Thickness made of Functionally Graded Materials. Composites: Part B. 2013; 45: 388–396p.
8. Nejad MZ, Jabbari M, Ghannad M. Elastic Analysis of Rotating Thick Truncated Conical Shells Subjected to Uniform Pressure Using Disk Form Multilayers. *ISRN Mech Eng*. 2014; 2014: 1-10.
9. Nejad MZ, Jabbari M, Ghannad M. A Semi Analytical Solution of Thick Truncated Cones using Matched Asymptotic Method and Disk form Multilayers. *Arch Mech Eng*. 2014; 61: 495–513p.
10. Afsar AM, Go J. Finite Element Analysis of Thermoelastic Field in a Rotating FGM Circular Disk. *Appl Math Model*. 2010; 34: 3309–3320p.
11. Seshu P. *A Text Book of Finite Element Analysis*. PHI Learning Pvt. Ltd.; 2003.
12. Kim JH, Paulino GH. Isoparametric Graded Finite Elements for Nonhomogeneous Isotropic and Orthotropic Materials. *ASME J Appl Mech*. 2002; 69: 502–514p.
13. Bayat M, Saleem M, Sahari BB, *et al*. Mechanical and Thermal Stresses in a Functionally Graded Rotating Disk with Variable Thickness due to Radially Symmetry Loads. *Int J Pres Ves Pip*. 2009; 86: 357–372p.

Cite this Article
Amit Kumar Thawait. Stress Analysis of Rotating Cylindrical Pressure Vessel of Functionally Graded Material by Element Based Material Gradation. *Research & Reviews: Journal of Physics*. 2016; 5(3): 7–15p.